Soil Water Content Distributions between Two Emitters of a Subsurface Drip Irrigation System

Maziar M. Kandelous*
Dep. of Environmental Sciences
Univ. of California–Riverside
Riverside, CA 92521
currently at
Dep. of Land, Air and Water Resources
Univ. of California–Davis
Davis, CA 95616

Jiří Šimůnek
Dep. of Environmental Sciences
Univ. of California–Riverside
Riverside, CA 92521

M. Th. van Genuchten
Dep. of Mechanical Engineering
Federal Univ. of Rio de Janeiro
Rio de Janeiro, RJ 21945-970, Brazil

Keyvan Malek
Dep. of Irrigation
Bu-Ali Sina Univ.
Hamedan, Iran

Subsurface drip irrigation (SDI) systems are increasingly being used in agriculture in attempts to use the available water more efficiently. The proper design and management of SDI systems requires knowledge of precise distribution of water around emitters. We conducted both field and numerical experiments to evaluate the soil water content distributions between two neighboring emitters when their wetting patterns started to overlap. The experiments involved SDI systems with emitters installed at different depths and with different spacings along the drip lateral. The HYDRUS software package was used to analyze the field data, assuming modeling approaches in which emitters were represented as (i) a point source in an axisymmetrical two-dimensional domain, (ii) a line source in a planar two-dimensional domain, or (iii) a point source in a fully three-dimensional domain. Results indicated that SDI systems can be accurately described using an axisymmetrical two-dimensional model only before wetting patterns start to overlap, and a planar two-dimensional model only after full merging of the wetting fronts from neighboring emitters. A fully three-dimensional model appears to be required for describing subsurface drip irrigation processes in their entirety.

Abbreviations: SDI, subsurface drip irrigation.

Subsurface drip irrigation systems are becoming increasingly popular as a means for supplying irrigation water, fertilizers, and pesticides more efficiently, and have been used on a range of vegetables, field crops, and fruit trees (Camp, 1998; Singh et al., 2006). Increasing the efficiency of water use is a major issue because competition between agricultural, municipal, and industrial users is likely to increase in the near future. As noted by Skaggs et al. (2004), realizing the full potential of subsurface drip technologies requires optimizing the operational parameters that are available to irrigators, such as the frequency and duration of irrigation, the emitter discharge rate and spacing, and the placement of the drip laterals. Thus, the proper design and management of SDI systems requires knowledge of the precise distribution of water around the emitters to provide an optimal distribution of water in the crop root zone without undue wetting of the soil surface and drainage to the groundwater.

During the past several decades, much research has been performed to describe water flow from point and line sources into the soil in order to design and efficiently manage SDI systems. This research included the development of both empirical and analytical models to describe soil water content patterns or wetting fronts for both surface and subsurface drip irrigation systems (e.g., Philip, 1968; Warrick, 1974; Schwartzman and Zur, 1986; Chu, 1994; Moncef et al., 2002; Cook et al., 2003). Due to increasing computer speed and the availability of more comprehensive numerical models for simulating flow in variably saturated soils, numerical approaches are now increasingly being used for evaluating water flow in SDI systems (e.g., Taghavi et al., 1984; Angelakis et al., 1993; Meshkat et al., 1999; Schmitz et al., 2002; Ben-Asher and Phene, 1996; Cote et al., 2003;

Soil Sci. Soc. Am. J. 75:488–497
Posted online 3 Jan. 2011
doi:10.2136/sssaj2010.0181
Received 26 Apr. 2010.
*Corresponding author (mkandelous@ucdavis.edu; mkandelous@gmail.com).

Skaggs et al., 2004; Lazarovitch et al., 2005, 2007; Provenzano, 2007; Kandelous and Šimůnek, 2010a,b). Several recent studies used for this purpose the two-dimensional version of HYDRUS (Šimůnek et al., 1999, 2006), which is a Microsoft Windows-based computer software package for simulating water, heat, and solute movement in both two- and three-dimensional variably saturated porous media. Some of these studies simulated the SDI process as an equivalent line source (a lateral) (e.g., Skaggs et al., 2004; Ben-Gal et al., 2004), while others approximated SDI by means of a point source (an individual emitter) (e.g., Provenzano, 2007; Lazarovitch et al., 2005, 2007; Kandelous and Šimůnek, 2010a,b). All of these studies were performed using either planar or axisymmetrical two-dimensional models, while in actuality SDI is a fully three-dimensional flow problem.

In this study, we addressed the types of errors that are made when a fully three-dimensional SDI flow process is approximated by an apparently two-dimensional process. Figure 1A shows simulated water content distributions in a three-dimensional SDI soil profile. For our simulations, we used a range of geometries and soil hydraulic properties, which are discussed below. Figure 1B illustrates that when water flow from a lateral is approximated as a two-dimensional process, it is assumed that water is discharged uniformly along the entire length of the lateral. Water is, in fact, discharged from individual emitters located along the lateral, while no discharge occurs from the lateral between neighboring emitters (Fig. 1A). Therefore, the assumption of two-dimensional flow is only an approximation of the real flow process. In fact, before the wetting patterns of two adjacent emitters begin to overlap (Fig. 1C), the three-dimensional flow process could be approximated well by an axisymmetrical two-dimensional process, and hence solved using a two-dimensional code like the two-dimensional version of HYDRUS (Šimůnek et al., 2006), the older HYDRUS-2D code (Šimůnek et al., 1999), or some other simulator. When two adjacent wetting patterns begin to overlap, however, the problem becomes a fully three-dimensional problem and hence needs to be solved using a three-dimensional numerical simulator. Depending on emitter spacing, irrigation duration, initial water content, and soil properties, the wetting patterns of two adjacent emitters will eventually overlap to a such extent that the water distribution between two emitters along a lateral becomes relatively uniform (Skaggs et al., 2004), as shown by plots IIA and IIB in Fig. 1. Only from this point onward can the flow process be approximated as a geometrically two-dimensional problem.

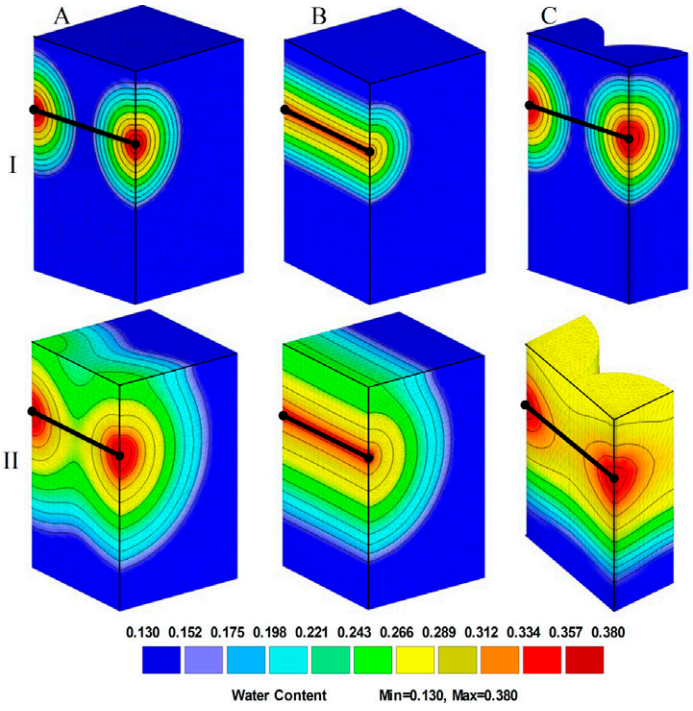

Fig. 1. Distribution of the soil water content in a subsurface drip irrigation system simulated as (A) a three-dimensional system with two point sources, (B) a two-dimensional system with a line source, and (C) an axisymmetrical two-dimensional system with a point source. Simulations with small (I, top) and large (II, bottom) amounts of applied water are shown.

Several of these SDI geometry issues were explored in detail in this study, both experimentally and numerically, using HYDRUS. The experimental studies produced soil water content distributions of SDI systems with emitters installed at different distances and depths. The observed water content distributions were compared with numerical simulations performed assuming approximate axisymmetrical two-dimensional and fully three-dimensional geometries. We also compared the results of hypothetical numerical simulations performed using planar two-dimensional, axisymmetrical two-dimensional, and fully three-dimensional geometries of the SDI system, with emitters installed at different depths and assuming different irrigation times, once they were calibrated to the experimental data.

The two main objectives of this study were (i) to validate HYDRUS-3D for modeling water movement in SDI systems by evaluating the measured soil water content distributions from several field experiments, and (ii) to compare simulated water content distributions for SDI systems with emitters installed at different depths and with different irrigation times using planar two-dimensional, axisymmetrical two-dimensional, and fully three-dimensional geometries and to discuss any possible differences.

MATERIALS AND METHODS

Field Experiments

Eight field experiments (Table 1) were performed at the research field of the College of Agricultural and Natural Resources of the University of Tehran, Iran, on a clay loam soil (32.5% clay, 36.5% silt, and 31.0% sand). Each experiment was conducted using two emitters installed at the same depth and having the same discharge rate. We used different emitter depths (20, 25, and 30 cm), which are typical of SDI systems for agronomic, turf, and tree crops (Camp, 1998). Spacings between two neighboring emitters along a lateral were 30, 40, and 45 cm, which are common for laterals produced by commercial irrigation companies. Finally, discharge rates commonly used in SDI systems were selected (e.g., Cote et al., 2003).

The field installation of the emitters used in this study was described in detail by Kandelous and Šimůnek (2010a). Water from a reservoir (consisting of a 160-mm-diameter polyvinyl chloride pipe) was delivered to the emitters with millimeter precision using a small pump. The volume of water in the water reservoir was recorded every

Table 1. Physical conditions for Experiments 1 through 8 in the field.

Parameter	1	2	3	4	5	6	7	8
Emitter installation depth, cm	25	30	25	20	30	30	25	25
Distance between emitters, cm	45	40	40	40	30	30	30	30
Discharge variation, $\times 10^{-3}$ m^3 h^{-1}	1.7–2.98	1.86–2.56	1.86–3.24	2.12–2.88	0.54–1.92	1.8–2.5	2.13–2.58	2.04–2.96
Discharge duration, min	300	359	473	450	363	276	450	335
Irrigation amount, $\times 10^{-3}$ m^3 (two drippers)	22.6	25.6	36.6	35.8	15.8	22.2	32.9	26.3

30 min to measure variations in the water discharge rate. The average discharge rate of individual experiments varied from 1.3×10^{-3} to 2.4×10^{-3} m^3 h^{-1}. Discharge rates gradually decreased during most irrigation experiments, probably due to the development of overpressure around emitter outlets (Lazarovitch et al., 2005). The emitter discharge variations, durations of irrigation, and the amounts of applied water are summarized in Table 1.

Soil surrounding the emitters was excavated immediately after each irrigation experiment to expose a vertical soil profile through a hypothetical lateral between two emitters for gravimetric soil water content measurements. Soil samples for this purpose were taken using a 3-cm-long steel soil sampler with a 3-cm inside diameter at locations 0, $d/4$, $d/2$, $3d/4$, and d centimeters away from the emitters (see Fig. 2), where d is the distance between two emitters, at the 10-, 20-, 30-, 40-, and 50-cm depths. In each case, 25 samples were collected by pressing the soil sampler horizontally into the soil profile at selected locations. Because the wetting patterns were presumably horizontally symmetric in the vertical plane between two emitters, samples taken at mirror positions were mixed after the individual sampling. Volumetric water contents were determined by multiplying the gravimetric water contents by the measured bulk density of 1.55 g cm^{-3}.

Except for the saturated water content, θ_s, the soil hydraulic parameters (van Genuchten, 1980) were initially estimated using the ROSETTA pedotransfer functions of Schaap et al. (2001) as implemented in the HYDRUS codes. The saturated water content was estimated directly in the laboratory using the collected field soil samples. To obtain better simulations of the field data, we further optimized the van Genuchten soil hydraulic parameter n, and the saturated hydraulic conductivity K_s, against the measured soil water contents using data from a control drip irrigation experiment by running the inverse parameter estimation option in HYDRUS. The control experiment and parameter optimization were described in detail by Kandelous and Šimůnek (2010a). The final estimated soil hydraulic parameters used in this study for the clay loam soil were: residual water content $\theta_r = 0.07$ m^3 m^{-3}, $\theta_s = 0.38$ m^3 m^{-3}, shape parameter $\alpha = 1.0$ m^{-1}, $n = 1.89$, $K_s = 5 \times 10^{-6}$ m s^{-1}, and shape parameter $l = 0.5$. The measured initial volumetric water content was 0.13 m^3 m^{-3}.

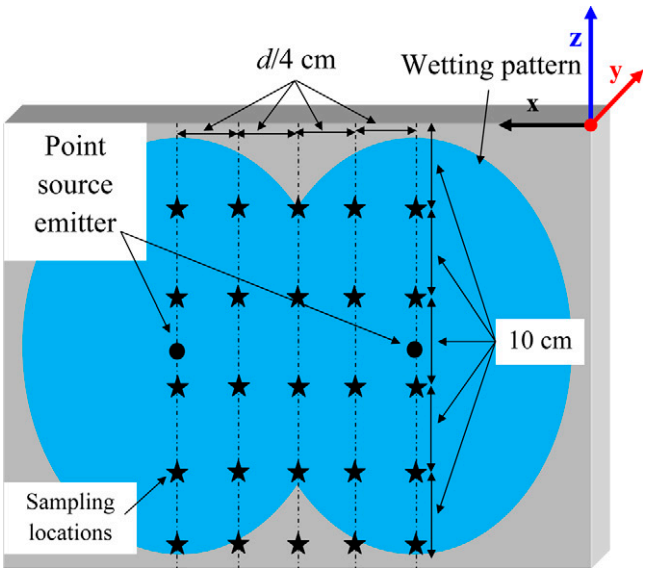

Fig. 2. Schematic of the field experimental setup, showing emitters and sampling distances, where *d* is the distance between emitters.

Numerical Experiments

Numerical flow experiments were performed considering different geometries of the SDI system. Soil water contents were simulated assuming laterals installed at the 20-, 30-, or 40-cm depth and located 100 cm apart, with emitter spacings of 50 cm (Fig. 3) and an emitter discharge rate of 1.60×10^{-3} m^3 h^{-1}. Irrigation in all simulations was applied during a 24-h period. Soil hydraulic parameters and the initial conditions used in all numerical experiments were the same as those used for the field experiments. Observation nodes (27 nodes) were located at nine depths between the soil surface and a depth of 80 cm (at intervals of 10 cm) and at three horizontal distances from the lateral (0, 12.5, and 25 cm) to obtain water contents at seven times (2, 4, 6, 8, 10, 12, and 24 h) for the statistical analysis comparing the numerical results obtained for the different SDI scenarios.

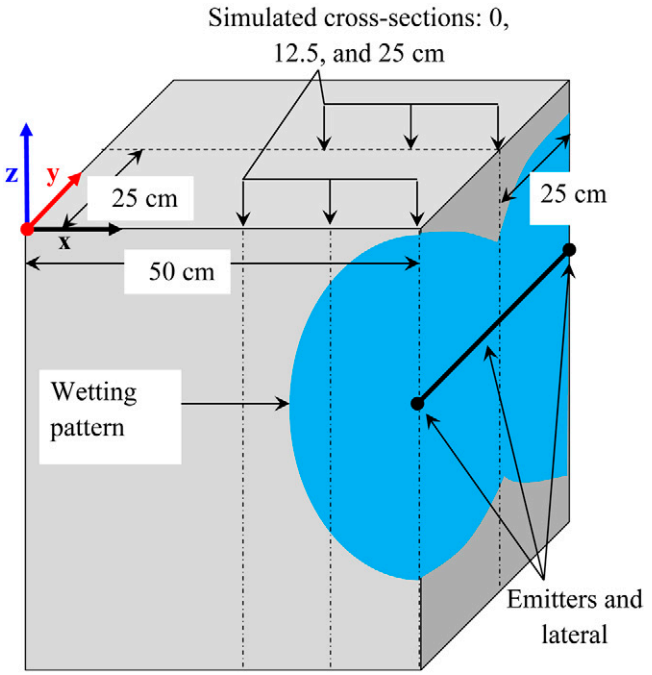

Fig. 3. Schematic of the flow domain used in the numerical experiments. The *x* and *y* axes are horizontal axes perpendicular and parallel to the direction of a lateral, respectively. The *z* axis is a vertical axis positive upward.

Water flow in the variably saturated SDI soil systems was described using the following modified form of the Richards equation:

$$\frac{\partial \theta}{\partial t}=\frac{\partial}{\partial x_i}\left[K\left(K_{ij}^{A}\frac{\partial h}{\partial x_j}+K_{iz}^{A}\right)\right] \quad [1]$$

where θ is the volumetric water content [L^3 L^{-3}], h is the pressure head [L], x_i (i = 1,2 for a two-dimensional model and i = 1,2,3 for a three-dimensional model) are spatial coordinates [L], t is time [T], K_{ij}^{A} and K_{iz}^{A} are components of the dimensionless anisotropy hydraulic conductivity tensor K^A (dimensionless), and K is the unsaturated hydraulic conductivity function [L T^{-1}] given by

$$K(h,x_i)=K_s(x_i)K_r(h,x_i) \quad [2]$$

where K_r is the relative hydraulic conductivity (dimensionless) and K_s is the saturated hydraulic conductivity [L T^{-1}]. The soil hydraulic properties were described using the van Genuchten–Mualem constitutive relationships (van Genuchten, 1980):

$$\theta(h)=\begin{cases}\theta_r+\dfrac{\theta_s-\theta_r}{\left(1+|\alpha h|^n\right)^m} & h<0\\ \theta_s & h\geq 0\end{cases} \quad [3]$$

$$K(h)=K_s S_e^l\left[1-\left(1-S_e^{1/m}\right)^m\right]^2 \quad [4]$$

where θ_s is the saturated water content [L^3 L^{-3}]; θ_r is the residual water content [L^3 L^{-3}]; α [L^{-1}], n, and l are shape parameters with m = 1 − 1/n; and S_e is the effective saturation, given by

$$S_e=\frac{\theta-\theta_r}{\theta_s-\theta_r},\quad m=1-\frac{1}{n} \quad [5]$$

For our studies, we assumed the soil to be isotropic, in which case the dimensionless anisotropy tensor, K^A, becomes a unit matrix (i.e., having values of one along the diagonal and zero values off-diagonal).

The governing flow Eq. [1] within HYDRUS was solved numerically using Galerkin-type linear finite elements (Šimůnek et al., 1999, 2006, 2008) in both two and three dimensions. This numerical scheme also allows a two-dimensional version of the Richards equation to be solved for three-dimensional problems exhibiting radial symmetry about the vertical axis (such as for flow from a point source). Because such problems involve only two coordinates (i.e., a vertical axis z and a radial axis r), we refer to these problems as axisymmetrical two-dimensional problems.

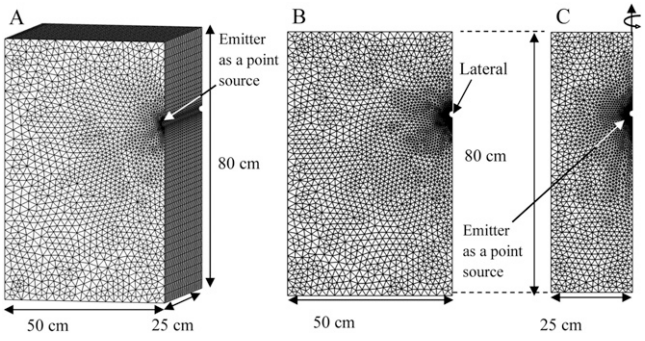

Fig. 4. Flow domains used in the numerical experiments and their discretizations assuming (A) a fully three-dimensional domain (P3D), (B) a planar two-dimensional domain (L2D), and (C) an axisymmetrical two-dimensional domain (P2D).

Possible Geometries of the Drip Irrigation System

As shown in Fig. 1, three different geometries could be applied to a SDI system: a fully three-dimensional system with two dripper sources (Fig. 1A), an approximate two-dimensional planar system involving a line source (Fig. 1B), and an approximate two-dimensional axisymmetrical system containing the dripper sources (Fig. 1C). Each is briefly discussed below.

Planar Two-Dimensional Geometry

The simplest approach assumes that the SDI system can be simulated using a planar two-dimensional model in which the lateral is represented as a point source in a two-dimensional domain (Fig. 1B). The dripper lateral is considered to be an infinite line source in a direction perpendicular to the simulated plane. This geometry has been used most frequently in numerical studies of subsurface drip systems (e.g., Skaggs et al., 2004; Ben-Gal et al., 2004; Gärdenäs et al., 2005; Lazarovitch et al., 2005,2007; Hanson et al., 2008; Elmaloglou and Diamantopoulos, 2009; Roberts et al., 2009). The line source model, referred to below as the L2D model (with L standing for line and 2D for two dimensions), was used only for the numerical experiments and not for analysis of the field data. The model is applicable to conditions in which the laterals are farther apart than the emitters along a lateral. In practice, this geometry can be used for conditions where the flow patterns from individual emitters overlap and merge to create a combined and relatively uniform flow pattern from an apparently single infinite line source (compare IIA and IIB in Fig. 1). Once this happens, the originally radially symmetrical (or axisymmetrical) two-dimensional or three-dimensional flow process can be simplified to an equivalent two-dimensional line source problem.

Because the flow field in a homogeneous subsurface drip irrigated field should be symmetric to the two vertical axes (planes) passing through the lateral and halfway between the two laterals, only half the space between two laterals needs to be simulated. The two-dimensional transport domain is thus rectangular and comprises half of the length between the two laterals (in our case 50 cm) and is 80 cm deep. A small semicircle on the right side of the transport domain represents the lateral (see Fig. 4B). The transport domain for our simulations was discretized into 4311 triangular finite elements, with their sizes gradually increasing with distance from the lateral. The smallest element around the lateral was about 0.1 cm, and the largest on the opposite of the domain was about 2 cm.

Axisymmetrical Two-Dimensional Geometry

A slightly more complicated geometry assumes that the SDI system can be simulated using an axisymmetrical (or radially symmetrical) two-dimensional model in which an individual emitter is represented as a point source located on the axis of rotation (Fig. 1C). This geometry has been used also in several SDI numerical studies (e.g., Provenzano, 2007; Kandelous and Šimůnek, 2010a,b). This geometry, referred to as the P2D model (with P standing for point and 2D for two dimensions), was used for both the field and numerical experiments. The model is primarily

applicable at early times when flow from any individual emitter can be considered to be radially symmetrical. Flow from each emitter remains axisymmetrical until the wetting patterns from neighboring emitters begin overlapping each other. After that, the axisymmetrical representation can only be an approximation of the fully three-dimensional problem insofar as the numerical results should increasingly depart from reality with increasing time and irrigation volume.

The transport domain for simulations using this geometry was again rectangular ($d/2$ cm wide and 80 cm deep, where d is the distance between emitters), except for a semicircle on the left side of the domain representing the dripper (see Fig. 4C, right side, and Fig. 5, left side). The transport domain for these simulations was discretized into between 2207 and 3268 triangular elements, depending on the width of the transport domain. Observation nodes for the numerical experiments were located at the same depths and radial distances from the source as in the planar two-dimensional model.

Full Three-Dimensional Geometry

Subsurface drip irrigation was also simulated using a fully three-dimensional model in which each emitter was considered as a point source. This model is referred to as the P3D model (P for point and 3D for three dimensions). This model, presumably the most realistic for actual field conditions, was used for analysis of the field data and for providing comparisons with the approximate planar and axisymmetrical two-dimensional models. Results obtained with this model should be identical to those for the axisymmetrical two-dimensional model during the early stages of the infiltration process. Once neighboring wetting patterns start to overlap or interact, however, flow becomes fully three dimensional, and only the three-dimensional model should be able to describe the complete infiltration process involving multiple overlapping wetting patterns.

Slightly different transport domains were simulated with this geometry when analyzing the field experiments in comparison to the numerical experiments. Field experiments involved only two emitters, while an infinite line of emitters was assumed for the numerical experiments. Hence, for the field experiments, we could not assume that flow was symmetrical about the y–z plane passing through the emitter (because there is the second emitter only on one side) but only about the x–z plane passing through the emitter and the y–z plane passing through the center between two emitters. The three-dimensional hexahedral domain representing half of the domain displayed in Fig. 2 was thus 50 + $d/2$ cm wide, 50 cm deep, and 80 cm high (Fig. 5, left), where d is the distance between two emitters. The emitter was located in the front plane of the flow domain. The domain was discretized into 70,000 to 140,000 three-dimensional triangular prismatic elements, with their sizes gradually increasing with their distance from the emitter.

For the numerical experiments, for which we assumed an infinite line of emitters, we could assume that flow was symmetrical about the y–z plane going through the emitters and about the x–z planes going through both the emitter and the middle between two emitters (see Fig. 3). As a result, the flow domain was 50 cm wide, 25($d/2$) cm deep, and 80 cm high (Fig. 4A) and discretized into 177,000 triangular prismatic three-dimensional elements, again with their sizes gradually increasing away from the emitter.

Observation nodes in the numerical experiments were, in each case, located at the same nine depths between the soil surface and a depth of 80 cm (with an interval of 10 cm) and at three horizontal distances from the lateral (0, 12.5, and 25 cm in the x direction) as those utilized in the two-dimensional simulations. Data were collected at two planes in the y direction, i.e., for y = 0 and 25 cm (see Fig. 3). The latter plane was used to evaluate the soil water content distributions in the plane between two emitters to show the effect of the two overlapping wetting patterns (see Fig. 3).

Boundary Conditions

A time-variable flux boundary condition was used along boundary elements representing the emitter during water application in simulations of the field experiment. A constant-flux boundary condition was used for the same purpose in the numerical experiments. The time-variable boundary fluxes represented the corresponding measured fluxes of the field experiments. These fluxes were calculated by dividing the quantities of water applied in 30-min intervals by the length or surface area of the boundary that represents an emitter in the HYDRUS model. A free-drainage boundary condition was applied along the bottom boundary. All the remaining boundaries were assigned a zero-flux boundary condition. A zero-flux condition was also used along the soil surface because evaporation could be neglected due to the presence of a plastic mulch during irrigation. Boundaries other than those along planes or axes of symmetry were assumed to be far enough away to not affect the flow dynamics in the domain.

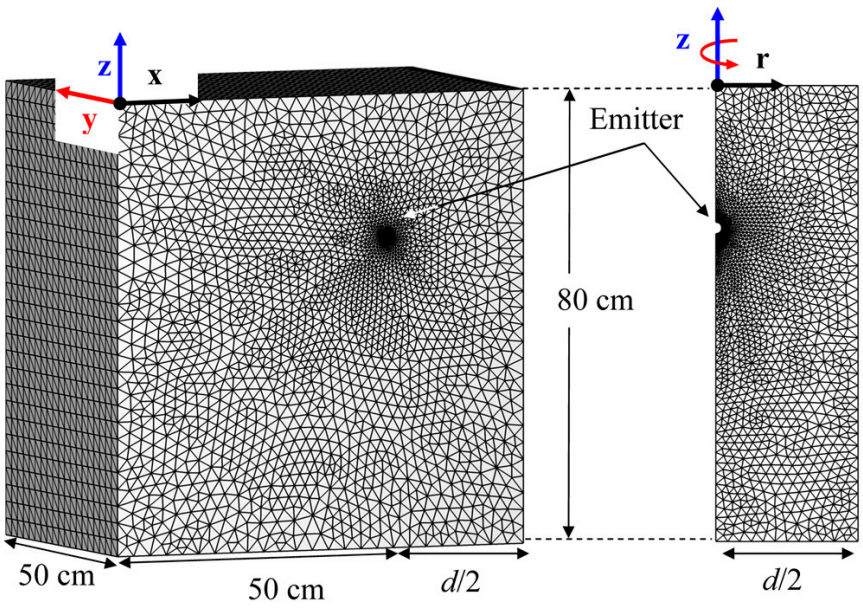

Fig. 5. Spatial discretization of the three-dimensional (left) and axisymmetrical two-dimensional (right) flow domains used for analysis of the field subsurface drip irrigation experiments, where *d* is the distance between emitters.

Statistical Analyses

Root mean square errors between the simulated and measured volumetric water contents, or between the simulated water contents obtained using different SDI geometries, were calculated to provide a quantitative comparison of the correspondence between the measured and simulated data or between the results of different models. The RMSE is given by

$$\mathrm{RMSE}=\sqrt{\frac{\sum_{i=1}^{n}(y_i-f_i)^2}{n}} \qquad [6]$$

where f_i and y_i are observed and simulated values, respectively, and n is the number of observations.

RESULTS AND DISCUSSIONS

Field Experiments

Figure 6 shows the measured and simulated soil water content distributions in a vertical plane between two neighboring emitters of a lateral for the eight field experiments with emitters installed at different depths and different spacings. Results are given for the distributions at the end of the infiltration experiments. Because of symmetry in the infiltration process, Fig. 6 shows only half of the area between the two emitters. Notice that the location of the dripper is indicated in each figure and that the size of each figure reflects the particular emitter spacing used in the various SDI experiments. The MATLAB 4 griddata method (e.g., Higham and Higham, 2005) was used to grid the measured water contents obtained at the sampling points. Subsequently, the contouring scheme of MATLAB was used to spatially interpolate the gridded water contents. Soil water content distributions were simulated for each field experiment using both the fully three-dimension (P3D) and axisymmetrical two-dimensional (P2D) versions of HYDRUS. The results in Fig. 6 show a qualitatively much better agreement between the measured and calculated distributions for the full three-dimensional simulations, especially for Exp. 3, 4, 7, and 8, which involved relatively large quantities of infiltrated water and hence showed more significant interactions between the individual moisture fronts.

The results in Fig. 6 are confirmed by the plots in Fig. 7, which show comparisons between the measured soil water contents at individual sampling points and those simulated using both the three-dimensional and axisymmetrical two-dimensional models at vertical transects 0, $d/4$, and $d/2$ away from the emitter, where d is the distance between two emitters along the lateral. The plots in Fig. 7 show that the three-dimensional model was able to describe the collected field data much better than the axisymmetrical two-dimensional model. This is especially true for those experiments (notably Exp. 3, 4, 7, and 8) that produced greater interaction between the moisture fronts coming from two neighboring emitters.

Table 2 summarizes the statistical results of comparisons between the measured and simulated water contents at the sampling points at the end of the infiltration experiments. Measured soil water contents are again compared with those simulated using both the three-dimensional (P3D) and axisymmetrical two-dimensional (P2D) models. The RMSE values characterizing differences between observed and simulated water contents using P3D varied between 0.017 and 0.031, and

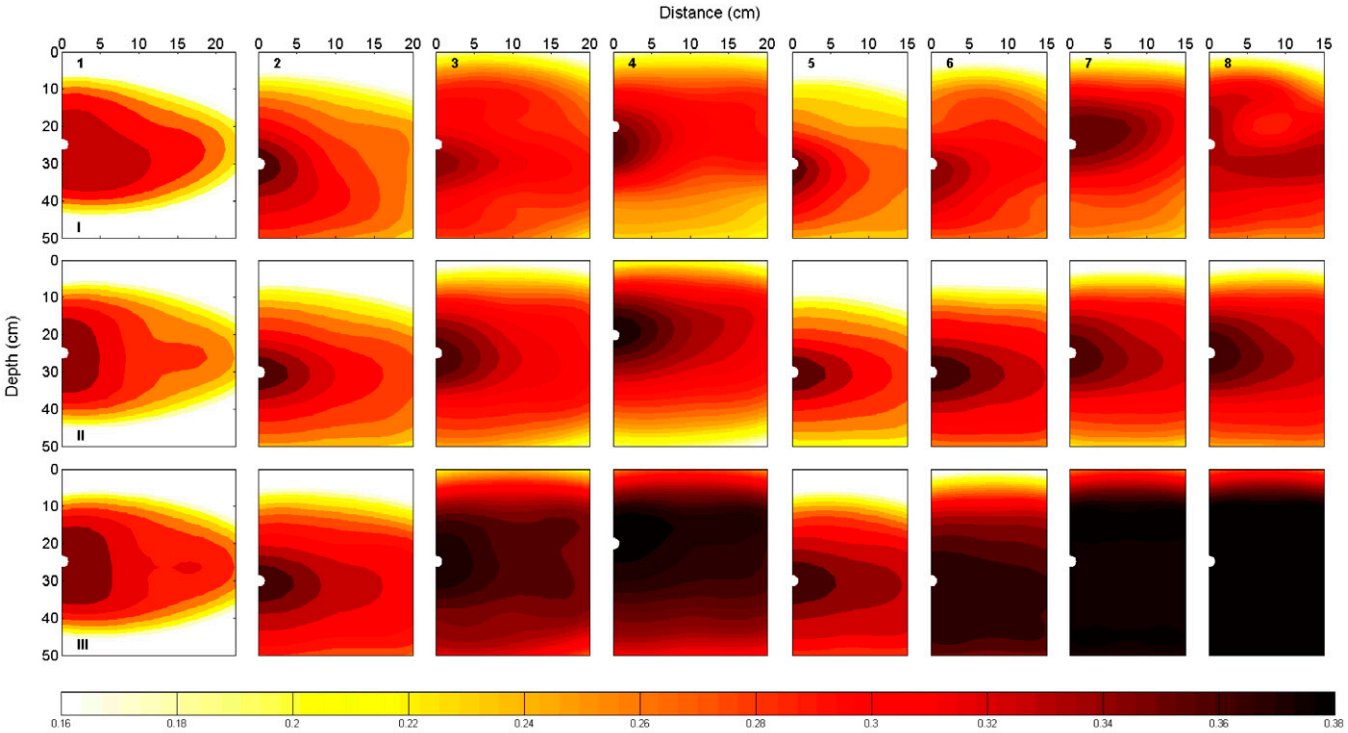

Fig. 6. Comparison of measured and simulated distributions of the volumetric soil water content ($m^3\ m^{-3}$) between two emitters for Experiments 1 to 8 (from left to right): measured (I, top); simulated using the three dimensional model (II, middle), and simulated using the axisymmetrical two dimensional model (III, bottom). The white semicircles indicate the location of a dripper.

between 0.026 and 0.087 for P2D. These values are very similar to the results reported by Skaggs et al. (2004) and Kandelous and Šimůnek (2010b) for their two-dimensional analyses.

The correspondence between the observed water contents and those simulated using the three-dimensional model was much better than with those simulated using the axisymmetrical two-dimensional model. For this reason, we used the three-dimensional simulations as our control and compared results obtained with the P2D model against results obtained using the P3D model. Table 2 shows that RMSE values for the differences between the P2D and P3D models varied from 0.018 to 0.087. The very low RMSE value of 0.018 for Exp. 1 was expected because the wetting patterns of the two neighboring emitters overlapped only slightly at the end of the simulations, thus reflecting the fact that the two models produced very similar results. Much larger RMSE values of 0.027, 0.052, and 0.072 were obtained for Exp. 2, 3, and 4, respectively, where emitters were installed 40 cm apart at decreasing depths. The larger RMSE values for the shallower experiments are a direct result of increasingly overlapping wetting patterns. Overlapping was caused in part by the longer duration of irrigation for emitters installed at shallower depths and in part by the failure of the wetting front to follow an axisymmetrical development when reaching the soil surface. The shallower installation depth of the emitters of Exp. 4, compared with Exp. 3, caused the wetting front to reach the soil surface much earlier, causing it to deviate increasingly from the predicted axisymmetrical distributions typical of P2D simulations.

For Exp. 5, 6, 7, and 8, in which the emitters were all installed 30 cm apart, the RMSE values were 0.052, 0.066, 0.080, and 0.087, respectively. These values also reflect the increased overlapping of the wetting patterns caused by greater quantities of applied irrigated water and consequently more substantial differences between two- and three-dimensional simulations. The larger quantity of applied water caused the RMSE to increase from 0.052 to 0.066 between Exp. 5 and 6. The larger RMSE value of Exp. 8 compared with Exp. 5 and 6 reflects the increasing effect of the soil surface because of the shallower emitter installation depth and the larger amount of applied water, both of which caused larger deviations between the two models.

Finally, as shown in Table 1, the amount of applied water in Exp. 7 was larger than that of Exp. 8, but the RMSE between the approximate P2D and complete P3D simulations was smaller. This is because the axisymmetrical P2D model predicted almost fully saturated soil profiles at the end of Exp. 8, contrary to the results gained with the three-dimensional model. The increased amount of irrigated water for Exp. 7, and thus the higher water contents predicted with the three-dimensional model, could then only further reduce deviations between the two simulations.

Finally, a word of caution on interpreting the statistical analyses of the simulation results. The statistical analyses were performed for water contents collected at the end of the infiltration experiments. As such, they pertain only to water content distributions at these particular times, and not the full transient flow process involved in getting to these final

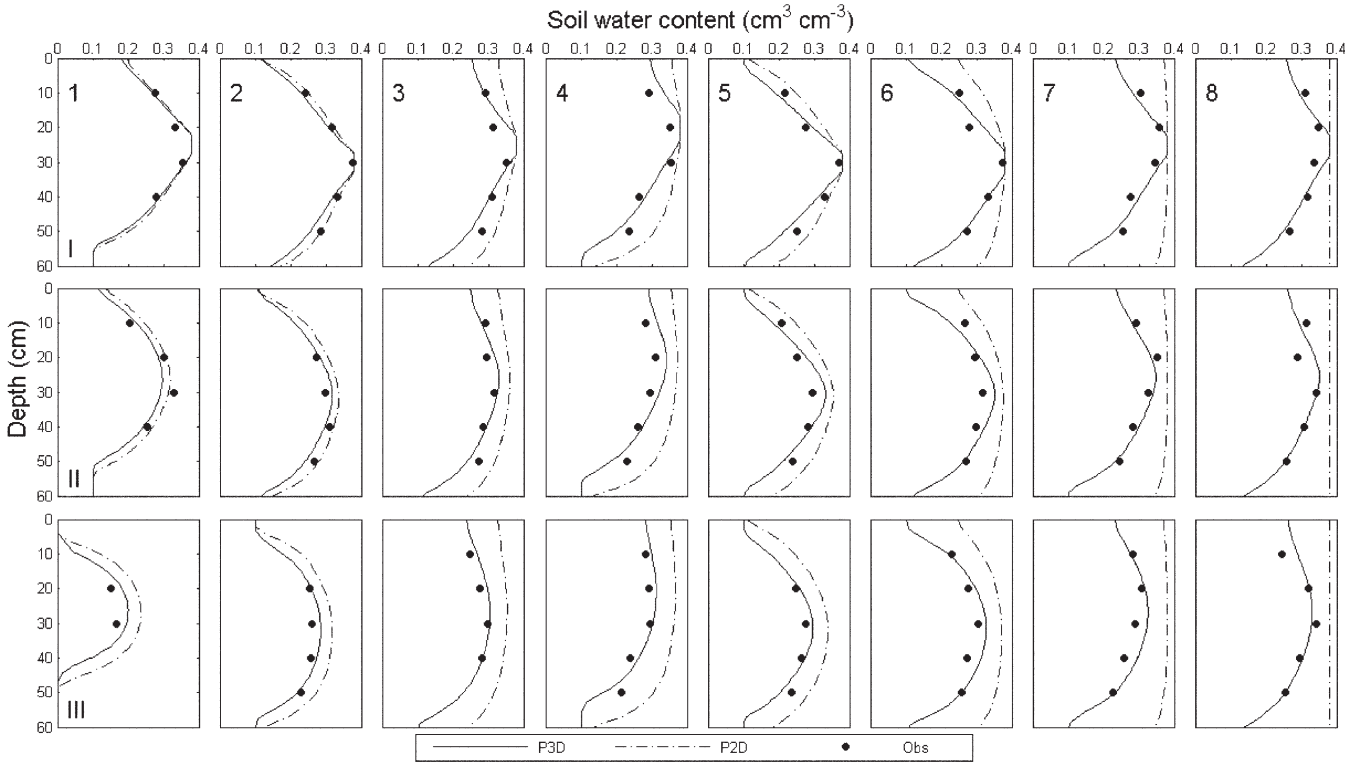

Fig. 7. Comparison of measured (dots) and simulated (lines) soil water contents between two emitters evaluated at locations involving different depths and distances from the emitter for Experiments 1 to 8 at the end of the irrigation experiment. The top (I), middle (II), and bottom (III) plots represent distanced of 0, *d*/4, and *d*/2 away from the emitter, respectively, where *d* is the distance between two emitters. Simulated results were obtained with the three-dimensional model (P3D, solid lines) and the two-dimensional axisymmetrical model (P2D, dashed lines).

Table 2. Statistical comparison of observed and simulated water contents at the end of the field infiltration experiments.

No.	Emitter depth	Emitter spacing	Irrigation amount	Comparison†	R^2	RMSE‡
	cm		$\times 10^{-3}$ m^3			
1	25	45	22.6	Obs. with P3D	0.82	0.021
				Obs. with P2D	0.84	0.026
				P3D with P2D	0.94	0.018
2	30	40	25.6	Obs. with P3D	0.85	0.017
				Obs. with P2D	0.80	0.027
				P3D with P2D	0.95	0.027
3	25	40	36.6	Obs. with P3D	0.68	0.022
				Obs. with P2D	0.57	0.053
				P3D with P2D	0.97	0.052
4	20	40	35.8	Obs. with P3D	0.82	0.031
				Obs. with P2D	0.75	0.074
				P3D with P2D	0.97	0.072
5	30	30	15.8	Obs. with P3D	0.85	0.025
				Obs. with P2D	0.82	0.048
				P3D with P2D	0.94	0.052
6	30	30	22.2	Obs. with P3D	0.80	0.026
				Obs. with P2D	0.62	0.069
				P3D with P2D	0.83	0.066
7	25	30	32.9	Obs. with P3D	0.64	0.023
				Obs. with P2D	NA§	0.080
				P3D with P2D	NA	0.080
8	25	30	26.3	Obs. with P3D	0.81	0.019
				Obs. with P2D	0.67	0.087
				P3D with P2D	0.90	0.087

† Obs, observed data; P3D, three-dimensional geometry; P2D, axisymmetric two-dimensional geometry.

‡ RMSE of calculated volumetric soil water contents.

§ NA, not applicable.

states. If the entire wetting process had been considered, then the statistical measures used to characterize the comparisons between the P2D and P3D simulations (notably R^2 or RMSE) would have been much better (larger and smaller, respectively) because the simulated wetting patterns during the early stages of infiltration would have been the same for the two models while producing differences only when neighboring wetting patterns started to interact.

Numerical Experiments

To provide greater insight into the effects of the assumed flow geometry on the resulting soil water content distributions in a subsurface drip irrigated field, a large number of simulations were performed with different emitter installation depths and emitter spacings along the SDI lateral. Soil water contents were simulated assuming three different geometric representations of the SDI system: a two-dimensional model (L2D), an axisymmetric two-dimensional model (P2D), and a three-dimensional model (P3D). The RMSE values were used to quantify the degree to which the two-dimensional models (L2D and P2D) approximated the results obtained with the three-dimensional model (P3D). The results for three different emitter installation depths are summarized in Table 3 for distributions in a vertical cross-section through the emitter perpendicular to the drip line. Figure 8 presents the calculated distributions for the three geometries for a single emitter installation depth of 30 cm. The results are for three vertical cross-sections 0, 12.5, and 25 cm away from, but parallel to, the dripper line.

Figure 8 indicates no discernable differences between the results obtained using the P2D and P3D models at early simulation times before the wetting patterns of two adjacent emitters began overlapping (after about 4 h). As the irrigation time increased, the wetting patterns began to overlap, causing them to mutually interact. From this point onward, water flow in the y direction along the lateral became different from water flow in the x direction perpendicular to the lateral. Water flow was then no longer radially symmetric, causing a divergence between the P2D and P3D results. This can also be demonstrated using the RMSE values in Table 3. These values were initially very small for all simulated depths because the results simulated for the P2D and P3D geometries were essentially identical. The RMSE values increased with time, however, as the assumption of radially symmetric flow was increasingly violated. As irrigation times increased from 2 to 24 h, the RMSE values increased from 0.002 to 0.118, from 0.002 to 0.098, and from 0.002 to 0.081 for installation depths of 20, 30, and 40 cm, respectively.

Different dynamics can be observed when comparing the results obtained using the L2D and P3D models (Fig. 8; Table 3). Notice that Fig. 8 presents two sets of lines for the P3D model. One line (denoted P3D1) represents the soil water contents in a plane perpendicular to the lateral at the emitter, while a second line (denoted P3D2) represents the water contents in a plane perpendicular to the lateral halfway between the two emitters. As expected, the water contents simulated using the L2D model are between those in the P3D1 and P3D2 planes (Fig. 8). While the L2D geometry led to only one line representing water contents along the entire lateral, the P3D geometry shows that soil water contents varied from maximum values in the P3D1 plane (at the emitter) to minimum values in the P3D2 plane (halfway between the emitters). At early times, water contents in the P3D2 plane remained at their initial values. An increase in water content in the P3D2 plane was always delayed in comparison with the P3D1 plane, at least during irrigation. As the irrigation time increased and the wetting patterns from two emitters started overlapping, differences between the water contents in the P3D1 and P3D2 planes were reduced again. Contrary to the gradually increasing RMSE values between the P2D and P3D results, the RMSE for differences between the

L2D and P3D models gradually decreased as the initially three-dimensional flow process became more two dimensional due to the overlapping moisture fronts. This is shown by the RMSE values for the differences between the L2D and P3D models, which decreased as the irrigation times increased from 2 to 24 h from 0.032 to 0.009, from 0.032 to 0.0108, and from 0.030 to 0.0091 for emitter installation depths of 20, 30, and 40 cm, respectively.

Table 3. Statistical comparison of simulated water contents at the end of the numerical infiltration experiments using different flow geometries and irrigation durations of 2 to 24 h.

Emitter depth	Scenarios used in the comparison†	RMSE‡						
		2 h	4 h	6 h	8 h	10 h	12 h	24 h
cm								
20	L2D vs. P3D1	0.032	0.030	0.026	0.022	0.017	0.014	0.009
	P2D vs. P3D1	0.002	0.006	0.016	0.027	0.036	0.044	0.118
30	L2D vs. P3D1	0.032	0.029	0.025	0.023	0.019	0.016	0.010
	P2D vs. P3D1	0.002	0.006	0.016	0.024	0.031	0.040	0.098
40	L2D vs. P3D1	0.030	0.025	0.024	0.022	0.018	0.016	0.009
	P2D vs. P3D1	0.002	0.006	0.015	0.023	0.030	0.038	0.081

† L2D, planar two-dimensional geometry representing the dripper as a line source; P2D, axisymmetrical two-dimensional model representing the emitter as a point source; P3D1, three-dimensional geometry representing each emitter as a point source along a lateral (values hold for a vertical cross-section through the drip lateral as shown in Fig. 3).

‡ RMSE of calculated volumetric soil water contents.

Figure 8 and the results in Table 3 indicate that water flow during the early stages of infiltration can be described well using the P2D model, with results essentially identical to the P3D results. As infiltration proceeded and the wetting fronts of the individual emitters started to overlap, the P2D results increasingly diverged from the P3D results. At that stage, only the fully three-dimensional model could describe the complex dynamics of the interacting moisture fronts between the emitters. As irrigation proceeded further, however, the P3D results started to resemble more and more the L2D results for an infinite line source. The P3D and L2D simulations eventually became nearly identical, with the water contents showing nearly uniform distributions along the lateral.

From the field and numerical experiments in this study, we conclude that the P2D simulations provided a good approximation of the actual SDI wetting patterns during the early stages of infiltration, while the L2D simulations were more realistic at later times. In general, however, the three-dimensional simulation provided more realistic results.

SUMMARY AND CONCLUSIONS

Eight SDI experiments, performed under field conditions, were used to follow and study in detail the development of initially separate and later overlapping wetting fronts stemming from neighboring emitters. The observed distributions were simulated using several geometry options available in the HYDRUS software package, i.e., axisymmetrical two-dimensional flow (P2D) and fully three-dimensional flow (P3D). Soil water contents were obtained from soil samples collected at various

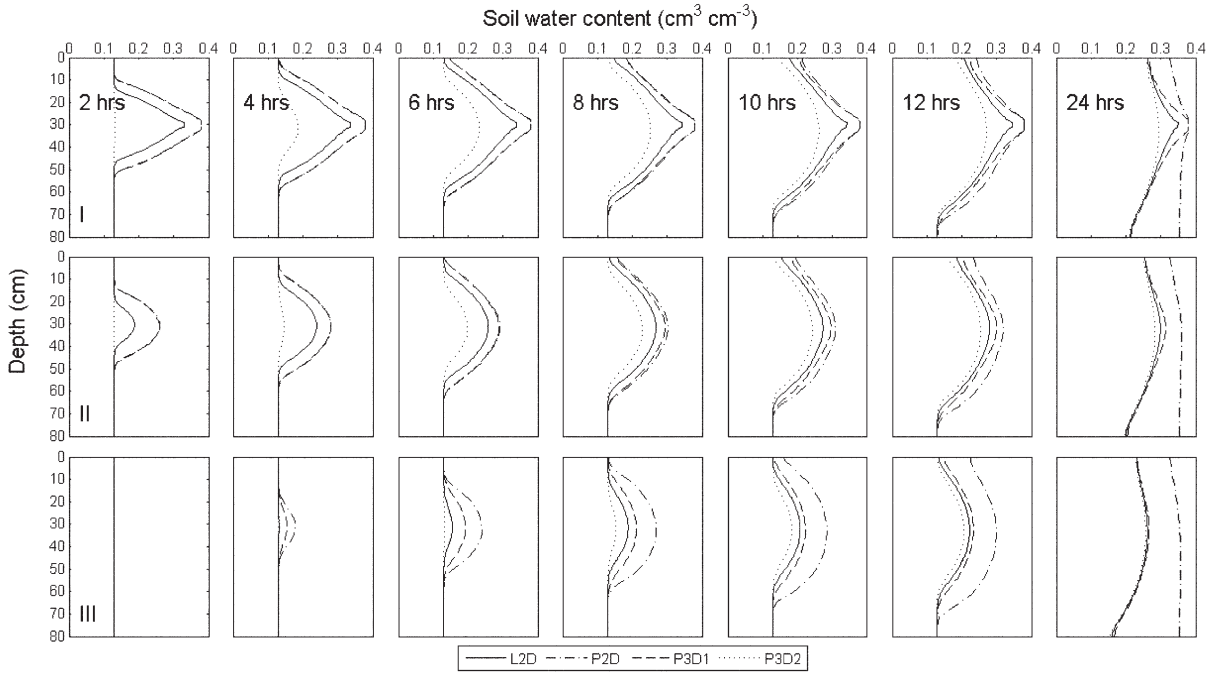

Fig. 8. Comparison of simulated soil water contents between two emitters obtained assuming three different subsurface drip irrigation domains. Water contents are shown for emitters installed at a depth of 30 cm for three distances away from the emitter. The top (I), middle (II), and bottom (III) plots represent distances of 0, 12.5, and 25 cm away from the drip line, respectively, and seven different irrigation times (left to right). Simulated results are for the planar two-dimensional geometry applicable to a line source (L2D, solid lines), axisymmetrical two-dimensional flow involving a point source (P2D, dashed dotted lines), and a three-dimensional domain with point sources (P3D1 for a cross-section across the drip line, dashed lines, and P3D2 for a cross-section halfway between two emitters perpendicular to the drip line, dotted lines).

locations from excavated soil profiles at the end of the irrigation experiments. The hydraulic parameters that provided the best fit were obtained using a combination of direct measurements, pedotransfer function predictions, and inverse analyses of the collected water content data.

Comparisons of the measured and simulated data showed that the three-dimensional HYDRUS model described the experimental data very well, providing levels of accuracy similar to those reported by Skaggs et al. (2004) for planar geometries and Kandelous and Šimůnek (2010b) for axisymmetrical two-dimensional geometries. Because of overlapping wetting patterns at the end of the infiltration experiments, the P2D model could not describe the collected water content data between two emitters as well as the three-dimensional model. A comparison of results obtained with the P2D and P3D geometries showed that the more the wetting patterns overlapped, the less successful the axisymmetrical two-dimensional model became in describing full three-dimensional subsurface irrigation processes.

We also conducted a series of numerical experiments to compare the results generated with the axisymmetrical (P2D) and planar (L2D) two-dimensional models with those obtained using the fully three-dimensional model (P3D). The results were compared at multiple irrigation times and for three different installation depths. The simulations showed that the axisymmetrical P2D model could predict water contents well during the early stages of infiltration before individual water patterns started overlapping, while the planar L2D model performed well at later stages of infiltration when the wetting patterns of individual emitters were fully merged. Only the fully three-dimensional model was able to describe the complex soil water SDI dynamics at all stages of the infiltration process.

We conclude that only the three-dimensional geometry provided accurate simulations of the water content for the assumed SDI system in a study involving multiple drippers, while two-dimensional axisymmetrical and line-source geometries provided good descriptions only before the wetting fronts started to overlap and after full merging of the wetting patterns, respectively. Ultimately, the HYDRUS code was found to be a very useful tool for studying the various SDI flow geometries and dynamic wetting patterns.

ACKNOWLEDGMENTS

This paper was based on work supported in part by the BARD (Binational Agricultural Research and Development Fund) Project IS-3823-06 and by the National Science Foundation Biocomplexity programs no. 04-10055 and NSF DEB 04-21530.

REFERENCES

Angelakis, A.N., T.N. Kadir, and D.E. Rolston. 1993. Time-dependent soil-water distribution under a circular trickler source. Water Resour. Manage. 7:225–235.

Ben-Asher, J., and C.J. Phene. 1996. Surface and subsurface drip irrigation: An analysis by a numerical model. Res. Rep. Jacob Blaustein Inst. for Desert Res., Ben Gurion Univ. of the Negev, Negev, Israel.

Ben-Gal, A., N. Lazarovitch, and U. Shani. 2004. Subsurface drip irrigation in gravel-filled cavities. Vadose Zone J. 3:1407–1413.

Camp, C.R. 1998. Subsurface drip irrigation: A review. Trans. ASAE 41:1353–1367.

Chu, S.T. 1994. Green–Ampt analysis of wetting patterns for surface emitters. J. Irrig. Drain. Eng. 120:414–421.

Cook, F.J., P.J. Thorburn, P. Fitch, and K.L. Bristow. 2003. WetUp: A software tool to display approximate wetting pattern from drippers. Irrig. Sci. 22:129–134.

Cote, C.M., K.L. Bristow, P.B. Charlesworth, F.J. Cook, and P.J. Thorburn. 2003. Analysis of soil wetting and solute transport in subsurface trickle irrigation. Irrig. Sci. 22:143–156.

Elmaloglou, S., and E. Diamantopoulos. 2009. Simulation of water dynamics under subsurface drip irrigation from line sources. Agric. Water Manage. 96:1587–1595.

Gärdenäs, A.I., J.W. Hopmans, B.R. Hanson, and J. Šimůnek. 2005. Two-dimensional modeling of nitrate leaching for various fertigation scenarios under micro-irrigation. Agric. Water Manage. 74:219–242.

Hanson, B.R., J. Šimůnek, and J.W. Hopmans. 2008. Leaching with subsurface drip irrigation under saline, shallow ground water conditions. Vadose Zone J. 7:810–818.

Higham, D.J., and N.J. Higham. 2005. MATLAB guide. 2nd ed. Soc. Ind. Appl. Math., Philadelphia, PA.

Kandelous, M.M., and J. Šimůnek. 2010a. Comparison of numerical, analytical and empirical models to estimate wetting pattern for surface and subsurface drip irrigation. Irrig. Sci. 28:435–444.

Kandelous, M.M., and J. Šimůnek. 2010b. Numerical simulations of water movement in a subsurface drip irrigation system under field and laboratory conditions using HYDRUS-2D. Agric. Water Manage. 97:1070–1076.

Lazarovitch, N., J. Šimůnek, and U. Shani. 2005. System-dependent boundary condition for water flow from subsurface source. Soil Sci. Soc. Am. J. 69:46–50.

Lazarovitch, N., A.W. Warrick, A. Furman, and J. Šimůnek. 2007. Subsurface water distribution from drip irrigation described by moment analyses. Vadose Zone J. 6:116–123.

Meshkat, M., R.C. Warner, and S.R. Workman. 1999. Modeling of evaporation reduction in drip irrigation system. J. Irrig. Drain. Eng. 125:315–323.

Moncef, H., D. Hedi, B. Jelloul, and M. Mohamed. 2002. Approach for predicting the wetting front depth beneath a surface point source: Theory and numerical aspect. Irrig. Drain. 51:347–360.

Philip, J.R. 1968. Steady infiltration from buried point sources and spherical cavities. Water Resour. Res. 4:1039–1047.

Provenzano, G. 2007. Using HYDRUS-2D simulation model to evaluate wetted soil volume in subsurface drip irrigation systems. J. Irrig. Drain. Eng. 133:342–349.

Roberts, T., N. Lazarovitch, A.W. Warrick, and T.L. Thompson. 2009. Modeling salt accumulation with subsurface drip irrigation using HYDRUS-2D. Soil Sci. Soc. Am. J. 73:233–240.

Schaap, M.G., F.J. Leij, and M.Th. van Genuchten. 2001. ROSETTA: A computer program for estimating soil hydraulic properties with hierarchical pedotransfer functions. J. Hydrol. 251:163–176.

Schmitz, G.H., N. Schutze, and U. Petersohn. 2002. New strategy for optimizing water application under trickle irrigation. J. Irrig. Drain. Eng. 128:287–297.

Schwartzman, M., and B. Zur. 1986. Emitter spacing and geometry of wetted soil volume. J. Irrig. Drain. Eng. 112:242–253.

Šimůnek, J., M. Šejna, and M.Th. van Genuchten. 1999. The HYDRUS-2D software package for simulating two-dimensional movement of water, heat and multiple solutes in variably saturated media. Version 2.0. IGCWMC-TPS 53. Int. Ground Water Model. Ctr., Colorado School of Mines, Golden.

Šimůnek, J., M. Šejna, and M.Th. van Genuchten. 2006. The HYDRUS software package for simulating two- and three-dimensional movement of water, heat, and multiple solutes in variably-saturated media. Technical Manual, Version 1.0. PC Progress, Prague, Czech Republic.

Šimůnek, J., M.Th. van Genuchten, and M. Šejna. 2008. Development and applications of the HYDRUS and STANMOD software packages and related codes. Vadose Zone J. 7:587–600.

Singh, D.K., T.B.S. Rajput, D.K. Singh, H.S. Sikarwar, R.N. Sahoo, and T. Ahmad. 2006. Simulation of soil wetting pattern with subsurface drip irrigation from line source. Agric. Water Manage. 83:130–134.

Skaggs, T.H., T.J. Trout, J. Šimůnek, and P.J. Shouse. 2004. Comparison of HYDRUS-2D simulations of drip irrigation with experimental observations. J. Irrig. Drain. Eng. 130:304–310.

Taghavi, S.A., M.A. Marino, and D.E. Rolston. 1984. Infiltration from a trickle irrigation source. J. Irrig. Drain. Eng. 110:331–341.

van Genuchten, M.Th. 1980. A closed-form equation for predicting hydraulic conductivity of unsaturated soils. Soil Sci. Soc. Am. J. 44:892–898.

Warrick, A.W. 1974. Time-dependent linearized infiltration: I. Point sources. Soil Sci. Soc. Am. J. 38:383–386.